2010

Charge Transfer and Nanostructure Formation During Electroless Etching of Silicon

Kurt W. Kolasinski

ohio2/yjy-yjy/yjy-yjy/yjy99907/yjy3755d07z | xppws | 23:ver.3 | 11/19/10 | 3:56 | Msc: jp-2010-08169b | TEID: brn00 | BATID: 00000

Charge Transfer and Nanostructure Formation During Electroless Etching of Silicon

Kurt W. Kolasinski*

Department of Chemistry, West Chester University, West Chester, Pennsylvania 19383, United States

Received: August 27, 2010; Revised Manuscript Received: November 5, 2010

The Turner mechanism of porous silicon formation during stain etching was developed and accepted without surface-sensitive data and without an understanding that nanostructures are being formed. Here it is shown that an oxide intermediate does not play a role in the formation of nanocrystalline porous Si films. Furthermore, a mechanistic understanding of etching and nanostructure formation leads to the formulation of seven rules for the rational design of stain etchants. These rules are used to develop three new formulations of stain etchants containing Fe^{3+}, VO_2^+, and Ce^{4+}, which are demonstrated to effectively produce porous silicon. These new formulations represent a significant advance in stain etching as they avoid many of the problems associated with common nitrate-/nitrite-based stain etchants including no need for "activation", short induction times, and the reproducible production of homogeneous films of unprecedented thickness.

I. Introduction

Nanostructured materials—thin films, nanoparticles, nanowires, and nanoporous solids—will play an important role in the development of advanced energy conversion and storage devices.[1−3] Such devices include photovoltaics, batteries, and fuel cells as well as materials for photocatalytic reactions, whether for hydrogen production or the production of other solar fuels by artificial photosynthesis. Porous Si (por-Si) and Si nanowires (SiNW) have appeared in numerous energy-related technologies. They are of growing interest to solar technology because of their potential to increase solar cell efficiency through (i) reduced reflectivity,[4−6] (ii) lower recombination losses,[7−10] and (iii) expanded spectral response.[11−13] A great deal of interest in por-Si has been in the areas of drug delivery[14,15] and sensors[16−18] as well as a variety of electronic and optoelectronic applications[19] and micromachining.[20−23] With proper chemical modification, por-Si and SiNW can form superhydrophobic surfaces[24−26] that can exhibit electrowetting behavior. Silicon has a significantly higher Li storage capacity than graphite; thus, it is promising as an anode in advanced battery designs. Use of por-Si can alleviate pulverization of the anode.[27,28] Large-area SiNW arrays are also promising for rechargeable lithium-ion battery anodes,[29] as well as in photoelectrochemical solar cells[30,31] and as gas sensors.[32]

Wet etching can produce both por-Si and SiNW. The hydrogen-terminated Si surface (H/Si) is important in the formation of both structures. As discussed by Kolasinski,[33] there are three electroless approaches to the formation of silicon nanostructured films: vapor phase etching, metal-assisted etching, and stain etching. All three can lead to por-Si formation, whereas SiNW production is only possible with metal-assisted etching. The formation of por-Si or SiNW by metal-assisted etching depends on whether the metal takes the form of an interconnected layer with openings in it or whether it is in the form of discrete nanoparticles. Dimova-Malinovska et al.,[34] Kelly and co-workers,[35,36] Bohn and co-workers,[37−40] Splinter et al.,[41] and Gorostiza and co-workers[42−44] have all studied the por-Si formation regime. Levy-Clement and co-workers[45] demonstrated that for etching in $HF/H_2O_2/H_2O$ solutions in the presence of Ag nanoparticles the HF to H_2O_2 concentration ratio is very important for determining whether micro- or macroporous Si is formed. Peng and co-workers[6,29−32,46−55] have performed extensive experiments to optimize film structures and have shown that ordered SiNW arrays can be formed with the aid of nanosphere lithography.[51]

Stain etching involves exposing Si to an aqueous mixture of acidic fluoride and an oxidant. Almost exclusively, the oxidant used is nitric acid (or another nitrate or nitrite). Robbins and Schwarz[56−58] and Turner[59] were the first to develop mechanisms. Robbins and Schwarz primarily studied the electropolishing regime, which results in a flat surface. Turner recognized the electrochemical nature of the process and that a pitted or porous film can be made if—rather than being uniform—the anodic and cathodic processes are (for some obscure and unexplained reason) localized at specific separate sites. These investigations led to the development of a mechanism that was based on scant evidence; nonetheless, it was accepted for stain etching virtually without question until the work of Nahidi and Kolasinski.[60]

The Turner mechanism consists of two steps: (1) oxidation of the Si surface to produce SiO_2 and (2) chemical removal of the SiO_2 layer (or patches) by HF attack.

$$\mathrm{Si} + 2\mathrm{H_2O} + n\mathrm{h}^+ \xrightarrow{\text{Step 1}} \mathrm{SiO_2} + 4\mathrm{H}^+ + (4-n)\mathrm{e}^- \xrightarrow{\text{Step 2: } + 6\mathrm{HF}} \mathrm{H_2SiF_6} + 2\mathrm{H_2O} \quad (1)$$

The role of the nitric acid is to inject holes in to the valence band (h^+_{VB}) via

$$\mathrm{HNO_3(aq)} + 3\mathrm{H}^+\mathrm{(aq)} \rightarrow \mathrm{NO(g)} + 2\mathrm{H_2O(l)} + 3\mathrm{h}^+_{\mathrm{VB}} \quad (2)$$

which leads to oxide formation and, importantly, the production of gas bubbles from NO(g).

A variation on the Turner mechanism has also been invoked to explain metal-assisted etching.[6,29,30,48−55,61,62] In these reports,

* Corresponding author. E-mail: kkolasinski@wcupa.edu.

10.1021/jp108169b

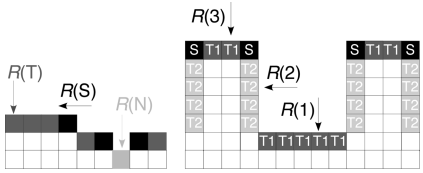

Figure 1. (a) Definition of the rate parameters important in step flow etching, roughening, and pore nucleation. (b) Definition of rate parameters controlling pore propagation. T denotes terrace sites, S step sites, and N a site on the next layer down.

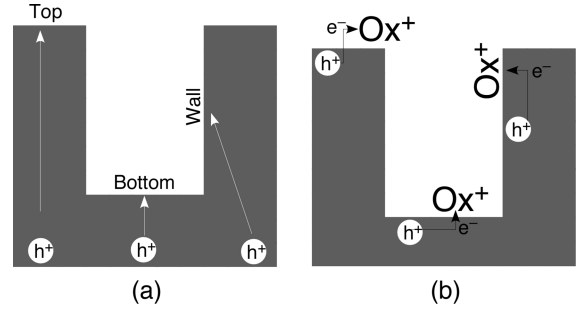

Figure 2. Electrochemical etching of Si initiated by the injection of holes h^+ into Si−Si backbonds at the surface. Regardless of whether etching is (a) anodic or (b) electroless involving an oxidant Ox^+, the holes need to be preferentially directed to the bottom rather than to the walls or top of the pore to ensure continued propagation.

it is proposed that the metal nanoparticles catalyze the formation of SiO_2 and that this SiO_2 film is removed by the chemical attack of HF. Close links between metal-assisted etching and stain etching can be surmised since it has been shown that metal-assisted etching can form not only etch tracks with a size similar to the diameter of the metal nanoparticle but also microporous silicon surrounding the etch tracks.[45,63,64] It should be noted that divalent Si atom etching, as opposed to the Turner mechanism, is accepted as the primary mechanism of Si atom removal during *anodic etching* in the porous silicon formation regime.[65] Nonetheless, oxide dissolution is important for anodic pore formation in models such as the current burst model.[66,67]

In this report, I consider all available evidence to formulate as complete a mechanistic understanding of stain etching as is currently possible. This understanding will significantly advance the usefulness of electroless etching as it is shown that rational formulation of stain etchants leads to nanocrystalline thin films, which exhibit superior reproducibility, homogeneity, and thickness compared to those obtained with conventional nitrate-based etchants.

II. Results and Discussion

Pore formation in crystalline materials, from a purely geometrical view of the chemistry of atom removal, contains inherent conflicts that seem to preclude its occurrence. As Figure 1(a) shows, there is good reason to believe that step flow etching should be the predominant mode of removing atoms from a surface. Step atoms are undercoordinated and should be easier to remove. In other words, the rate of step atom etching R(S) should exceed that of terrace atom etching R(T). This will always lead to *flat surfaces*. Roughening of the surface occurs when the rates of these two processes are roughly equal, R(S) $\approx R$(T). However, pore formation requires that the rate at which an atom from the next layer (the layer exposed when a terrace atom is removed) R(N) should exceed R(T) and R(S). From a steric viewpoint, this appears to be impossible. Consequently, pore nucleation likely is always preceded by roughening, which tends to make the distinction between T, S, and N sites less well-defined. Statistical fluctuations in the surface structure eventually lead to an appropriate geometry for pore nucleation from which pore propagation ensues.

Figure 1(b) shows the kinetic requirements for pore propagation. Pore propagation requires that the pore bottom etches significantly more rapidly than the pore walls $R(1) > R(2)$ and more rapidly than the top of the pores $R(1) > R(3)$. Again, on purely steric grounds, this seems highly unlikely since exactly the same sites may be present at the top and bottom of the pore and possibly on the walls depending on crystallography. It therefore appears unlikely that pore formation will occur in a single-crystal system etched by purely chemical means.

However, if the etching reaction responds to electric fields or the electronic structure of the solid, pore formation can be induced.[68] Electrochemical reactions obviously meet these criteria, and indeed, we find pore formation and nanostructure formation to be widespread under appropriate conditions for electrochemical processes whether anodic[67,69−71] or electroless.[33] At least two different effects can be identified which can naturally direct reactivity to the bottoms of the pores while effectively passivating the walls and tops. We can understand this with the aid of Figure 2. First, consider Figure 2(a), the case of anodic pore etching in which carriers are created in the bulk of the material and transported under the influence of an electric field to the reactive interface. The etching of Si is induced by holes. If the electric field is inhomogeneous and stronger at the pore bottoms, then the field will shepherd the carriers responsible for initiating reactivity to the bottom of the pores. A greater concentration of carriers at the bottom leads to a greater etch rate and ensures pore propagation. The second effect, proposed by Lehmann and Gösele,[72] is quantum mechanical in nature. If the pore walls become narrow enough (smaller than the exciton radius), quantum confinement shifts the band gap of the semiconductor by forcing down the valence band maximum and forcing up the conduction band minimum. Holes approaching from the bulk would then be directed by band bending toward the bottom of the pores.

Figure 2(b) treats the case of electroless etching initiated when an oxidant specifically adsorbed on the surface of the semiconductor accepts an electron and thereby injects a hole into the valence band. Since diffusion of the species in solution leads to equally probable collisions over the entire surface of the porous material, simple transport properties cannot be responsible for the anisotropic injection of holes preferentially at the bottom and to the exclusion of the walls and tops. In fact, reaction-induced depletion of a solution species can occur at the bottom of the pore if the reaction is faster than the diffusion of the oxidant, which is just the opposite of what is necessary to maintain pore propagation.

Only the quantum confinement effect can explain the preferential injection of holes into the bottom of the pores at the expense of the walls and tops during electroless etching. To understand this, we need to calculate the dependence of the charge transfer probability as a function of the wall thickness. The equilibrium electron transfer current via the valence band is given by[73]

$$i_{v0}^{-} = k_v^{-}(N_V - p_s^0)N_{ox} \exp[-(E_{ox}^0 - E_V)^2/4\lambda k_B T] \quad (3)$$

where the critical parameters are the reorganization energy λ, oxidant concentration N_{ox}, position of acceptor level E_{ox}°, position of the valence band maximum (VBM) E_V, and absolute

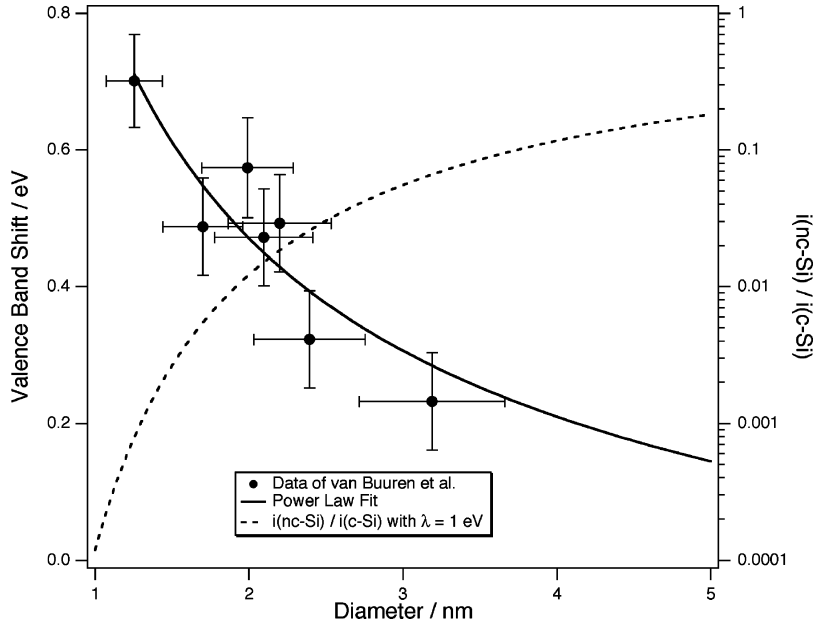

Figure 3. Data points on valence band shift in nanoscale silicon from van Burren et al.[74] fitted to a simple power law and used to calculate the decrease in the hole injection rate into Si nanostructures induced by an oxidant relative to bulk crystalline Si.

temperature. In addition, k_B is the Boltzmann constant; k_v^- is a rate constant; N_V is the density of states at the valence band edge; and $p_V°$ is the concentration of holes at the surface. What is important to note in eq 3 is that E_V is a function of Si nanocrystallite size. This is shown in Figure 3 from the data of van Buuren et al.[74] The valence band shift ΔVB follows the form

$$\Delta VB = B + Ad^{-n} \tag{4}$$

To fit the data, a point was added at (d = 9.8 nm, ΔVB = 0), and B is set to zero to ensure that quantum confinement goes to zero above the diameter of the Si exciton.[75] A weighted fit constrained by $B = 0$ yielded $A = 0.93 \pm 0.11$ eV, and $n = -1.04 \pm 0.18$ and fitted the data well as can be seen in Figure 3.

Assuming that the valence band shift is not accompanied by any change in the density of states or surface hole concentration, eqs 3 and 4 allow us to calculate the ratio the electron transfer rate in nc-Si to that of bulk crystalline Si (c-Si) as a function of the nanocrystallite diameter according to

$$\frac{i_{nc\text{-}Si}^-}{i_{c\text{-}Si}^-} = \exp\left[\frac{\Delta VB(2E_V - 2E_{ox}^0 - \Delta VB)}{4\lambda k_B T}\right] \tag{5}$$

The value of the reorganization energy λ is not known exactly but is on the order of 1 eV.[76] Values of the relative electron transfer rate $i_{nc\text{-}Si}^-/i_{c\text{-}Si}^-$ are plotted in Figure 3 for V_2O_5 acting as the oxidant.

In summary, therefore, stain etched films are composed of nanoscale pore walls that are connected to the substrate as opposed to an agglomeration of nanoscale particles because of the self-limiting nature of Si etching and the influence of quantum mechanical effects on carrier transport. Holes are injected into bulk silicon with the highest rate rather than into the walls or tips of the pores. Furthermore, quantum confinement reduces the diffusive transport of holes from the bulk into the pore walls. Therefore, the films preferentially form connected structures rather than particles.

In passing, it is noted that the charge transfer probability for a molecule approaching a surface at the gas/surface interface has been the subject of intense study, particularly in connection with nonadiabatic processes at surfaces.[77] From this work, the electron transfer probability is proportional to $\exp[-(E_V - E_{ox}^0)/\omega_0]$ rather than $\exp[-(E_{ox}^0 - E_V)^2/4\lambda k_B T]$. While this functional form is different, the effect on the etch rate is the same. It decreases with increasing slope as the diameter decreases.

It is instructive to consider the thermodynamics of Si and SiO_2 etching. This is shown in Figure 4 below. The enthalpies of formation of all compounds are taken from the CRC handbook,[78] except for that of H_2SiF_6.[79] The activation energy for SiO_2 etching is estimated from Judge.[80] There is no good experimental value of the thermal activation energy for HF etching of Si; therefore, a value is estimated from theoretical calculations.[81] The etch rates of Si[82,83] and SiO_2[84] are also available in the literature.

It is, of course, well-known that SiO_2 is not stable in the presence of HF(aq) both because there is a very small activation barrier and because the reaction is strongly exothermic. Si is not thermodynamically stable in the presence of water compared to SiO_2, nor is it thermodynamically stable with respect to H_2SiF_6 in the presence of HF. The appreciable (~2220 Å min^{-1}) etch rate of SiO_2 adheres to expectations. However, the vanishingly small etch rate of Si (~0.5 Å min^{-1}) does not. This means that neither H_2O nor HF reacts with Si with an appreciable rate at room temperature. The Si surface is H-terminated (H/Si), as shown by Ubara et al.[85] and Chabal and co-workers.[86] The hydrogen termination creates a significant kinetic barrier to both oxidation by H_2O and etching by HF. The reaction rate can be increased by increasing the pH because OH^- is able to catalyze the reaction of water with the surface.[87−89] Similarly, boiling water has both a great deal of thermal energy and a significantly increased concentration of OH^-, both of which enhance the etch rate.[90] In both cases, step flow etching occurs, and uniform surfaces result.[91] This is strong evidence that oxide films or patches never form during alkaline or boiling water etching because these solutions do not etch

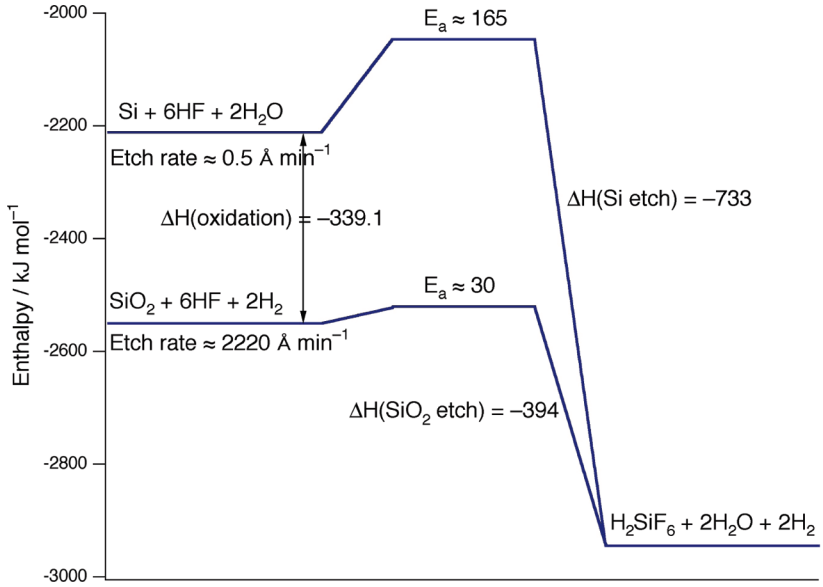

Figure 4. Reaction energy profiles for Si and SiO_2 etching in terms of the enthalpies of products and reactants with estimates of the thermal activation barriers for the two reactions.

the oxide at an appreciable rate; consequently, oxide patches would arrest etching, contrary to experimental evidence. Hydroxide induced etching is even involved in the formation of flat surfaces in the presence of F^-.[92−96] The mechanisms of fluoride etching and hydroxide etching are almost identical; therefore, it is implausible that oxide formation is involved in fluoride etching.

It thus behooves us to perform the surface science experiment to determine whether oxide films form during stain etching. The Turner mechanism calls for the formation of SiO_2 films or patches—not isolated adsorbed OH units and not individual adsorbed O atoms. No conclusive evidence for oxide film formation during por-Si production has been obtained in the ensuing years, and the most recent X-ray photoelectron spectroscopy measurements[97−102] as well as our own FTIR measurements[103,104] of the Si surface after stain etching revealed the absence of SiO_2. No reasoning for how a perfectly isotropic reaction such as chemical removal of SiO_2 can lead to por-Si formation, which requires *a great deal of anisotropy and a self-limiting reaction*, is contained in the Turner mechanism. This mechanism is woefully inadequate to explain stain etching and por-Si formation.

The one major difference between alkaline and fluoride etching is in the all important initiation step.[104,105] The implications of this are dramatic. Alkaline etching is extremely anisotropic: different planes etch at very different rates, and etching occurs almost exclusively at steps rather than on terraces. Fluoride etching of Si does not exhibit this degree of anisotropy when initiated by free carriers: there is little difference from plane to plane, and both step and terrace sites are attacked. Alkaline solutions destroy por-Si and produce flat surfaces. Acidic fluoride solutions etch Si to produce comparatively rough surfaces and can create por-Si.

In an acidic fluoride solution, the primary means of initiating reactivity is to inject a hole into the valence band of Si. The hole can be injected by an applied bias, through photon absorption or by collision with an oxidant.[33,92,104] The injected hole is transported to a Si−Si backbond where it raises the reactive sticking coefficient of F^- by 10 orders of magnitude.[92]

As a final proof that an oxide intermediate is not involved in por-Si formation during etching, let us consider bubble formation during etching. The overall reactions for the Turner mechanism are written as follows

$$\text{Initiation} \quad \mathrm{Si + 4Ox^+ \rightarrow Si^{4+} + 4Ox} \qquad (6.1)$$

$$\mathrm{SiO_2\ formation} \quad \mathrm{Si^{4+} + 2H_2O \rightarrow SiO_2 + 4H^+} \qquad (6.2)$$

$$\text{Chemical etching} \quad \mathrm{SiO_2 + 6HF \rightarrow H_2SiF_6 + 2H_2O} \qquad (6.3)$$

$$\text{Sum} \quad \mathrm{Si + 4Ox^+ + 6HF \rightarrow H_2SiF_6 + 4Ox + 4H^+} \qquad (6.4)$$

Ox^+ is the oxidant, and Ox represents its reduced form. Note that this reaction creates no H_2 and that the only bubbles that can form would be associated with the reduction $4Ox^+ + 4e^- \rightarrow 4Ox$. Bubbles created by this heterogeneous reduction would have to appear on the surface where etching occurs because that is where the charge transfer has to occur. However, Kooij et al.[106] have shown that during etching in HNO_3 + HF roughly 80% of the gas released is H_2 not NO or other nitrogen oxides.

Silicon atom removal via the Gerischer mechanism can be written

$$\text{Initiation} \quad \mathrm{Si + Ox^+ \rightarrow Si^+ + Ox} \qquad (7.1)$$

Fluoride etching $Si^+ + 3HF_2^- \rightarrow HSiF_3 + 2H^+ + 3F^- + e^-$ (7.2)

Product Rxn $HSiF_3(aq) + 3HF(aq) \rightarrow H_2SiF_6(aq) + H_2(g)$ (7.3)

Sum $Si + Ox^+ + 3HF + 3HF_2^- \rightarrow H_2SiF_6 + 2H^+ + H_2 + 3F^- + e^- + Ox$ (7.4)

Counter Rxn $H^+ + e^- \rightarrow 1/2H_2$ (7.5)

Fluoride etching, written with HF_2^- rather than HF since the former is roughly 15× more reactive,[107] releases a conduction band electron, which must be consumed in a counter reaction. Because this electron is mobile, the counter reaction does not have to occur where the electron is injected. The counter reaction can occur remotely. The product reaction also releases H_2; however, this can occur in solution away from the surface. If no gas production is associated with the reduction of Ox^+, the only gas produced is H_2, and 3/2 mol of H_2 is produced for every mol of Si etched. When HNO_3 is used, various reductions result in the production of NO_x, for example, $HNO_3 + 3H^+ + 3e^- \rightarrow NO + 2H_2O$. This corresponds to a 4.5:1 ratio of H_2 to NO_x, close to the 4:1 ratio observed by Kooij et al., consistent with reaction scheme 7 but inconsistent with reaction scheme 6.

Kolasinski and co-workers[60,103,108,109] have shown that the oxidant must have a standard electrode potential roughly more positive than +0.7 V to inject a hole into the valence band of conventionally doped Si. On this basis (and in accord with rules that will be delineated below), Kolasinski and co-workers have demonstrated quite reproducible and facile por-Si production with the use of three different oxidants, which do not generate gas during their reduction. These are Fe(III), Ce(IV), and V(V), which are reduced according to

$$Fe^{3+} + e^- \rightarrow Fe^{2+} \qquad E_0 = 0.77\ V \tag{8}$$

$$Ce^{4+} + e^- \rightarrow Ce^{3+} \qquad E_0 = 1.4\ V \tag{9}$$

$$VO_2^+ + H^+ + e^- \rightarrow VO^{2+} + OH^- \qquad E_0 = 1.0\ V \tag{10}$$

There are reports that stain etched films are limited to 1 μm thickness.[65] This is not true for stain etchants made from $FeCl_3 \cdot 6H_2O$ or V_2O_5. We have previously reported thick por-Si films of >10 μm using Fe^{3+} (ref 109). In Figure 5, it can be seen that a thickness of ~20 μm has been achieved by etching for 60 min in 0.22 M V_2O_5 in 50% HF at room temperature. These por-Si films are unusually thick compared to stain etching with HNO_3. In some cases (see table-of-contents image) these films can exhibit signs of exfoliation caused, as described previously,[109−111] by drying-induced stresses. Exfoliation can be avoided by critical point drying.

During etching with these oxidants, bubbles form, consistent with H_2 production according to the Gerischer mechanism, reaction scheme 7. However, Si is a terrible catalyst for H_2 formation; therefore, bubbles initially form on the edges of the crystal and scratches on the crystal face. The bubbles do not form uniformly across the crystal face as is seen with HNO_3 + HF. At long etch times when the films become quite thick, bubbles gradually begin to build up across the surface. This is caused by the increasing resistivity of the por-Si film and the difficulty of transporting electrons out of the film to the edges. It is well-known that the nanocrystalline nature of por-Si increases its resistivity.[112] In conclusion, the pattern of bubble formation is clearly consistent with the Gerischer mechanism and in direct opposition to a mechanism involving an oxide intermediate.

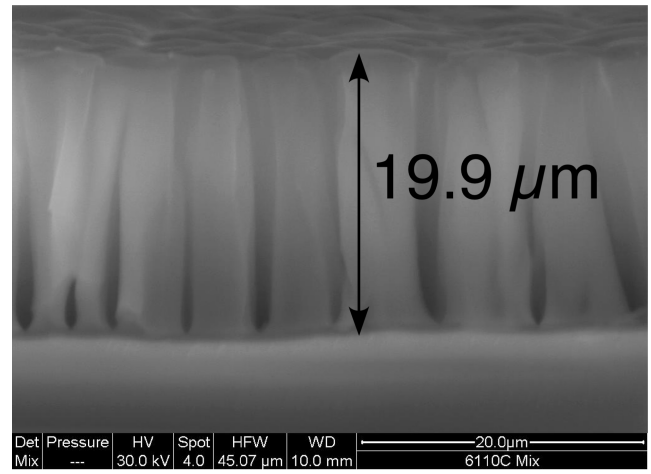

Figure 5. Scanning electron micrograph of a porous silicon film etched for 60 min and 0.22 M in V_2O_5 in 50% HF(aq).

It is well-known in anodic etching that if the bias is turned up too high etching makes a transition from pore formation to electropolishing, which must result from a change in the balance of surface reactions.[113] The thickness of the oxide can exhibit oscillations,[114−116] and the structure of the oxide and the nature of the oscillations has provoked active study.[117,118] Similarly for stain etching at too high a concentration of oxidant, electropolishing is observed. Even in metal-assisted etching, at very high H_2O_2 concentration relative to HF, polishing is observed.[45] If the Gerischer mechanism is the primary means of Si atom removal, is there any way that a transition from pore formation to electropolishing can occur?

Below I will develop a simple kinetic argument, which demonstrates that a shift from porous film production to electropolishing is plausible. No attempt is made to determine the structure of the substrate when passing through or after this transition. Whether roughening or electropolishing occurs will depend on the extent of the oxide before it is removed. However, pore propagation in the presence of oxide growth is only possible if oxide formation is confined to the tip of the pore. Electropolishing will occur when a substantial oxide layer is formed; however, as the studies on current oscillations mentioned above demonstrate, the nature of this transition and its structural effects are complex.

Above, it has already been established that an acidic fluoride solution is advantageous for a stain etchant since the low pH suppresses step flow etching that would accompany an appreciable concentration of OH^-. In the absence of OH^- to catalyze its dissociation, there is no way for water to dissociate on the H/Si surface because dissociative adsorption requires two empty sites. The adsorption of F^- only requires one excited site (a site excited by the hole injected into the valence band). Kolasinski[92] has demonstrated based on energetics that the hole cannot lead directly to desorption of adsorbed H atoms and the formation of an empty site; however, I suggested that the first

ohio2/yjy-yjy/yjy-yjy/yjy99907/yjy3755d07z | xppws | 23:ver.3 | 11/19/10 | 3:56 | Msc: jp-2010-08169b | TEID: brn00 | BATID: 00000

F^- ion to hit the surface creates an empty site through an abstraction reaction. If this is true, then the number of empty sites on the surface will be directly proportional to the number of holes injected. F^- adsorption is first order in the number of empty sites θ^* and, therefore, first order in the number of holes injected. Water adsorption will be second order in the number of empty sites and the number of holes injected. The same kinetics would also be followed if F^- adsorption only occurs at a site with a single excitation and if water requires two adjacent excited sites. It remains to be proved whether water dissociation requires two adjacent empty sites or two adjacent excited sites; nonetheless, the kinetics is second order in both cases.

Because of the different reaction orders, F^- adsorption is heavily favored at low empty site coverage (low hole injection rates), whereas water dissociative adsorption (and therefore oxide formation) is favored at high empty site coverage (high hole injection rates). The rates of F^- and water adsorption R_F and R_w, respectively, can be expressed as (assuming kinetic rather than diffusion control)

$$R_F = s_F c_F \left[\frac{k_B T}{2\pi m_F}\right]^{1/2} \theta^* \tag{11}$$

$$R_w = s_w c_w \left[\frac{k_B T}{2\pi m_w}\right]^{1/2} (\theta^*)^2 \tag{12}$$

s_F, s_w, c_F, c_w, m_F, and m_w are the sticking coefficients and masses of F^- and H_2O, respectively; θ^* is the fractional coverage of empty (or excited) sites; k_B is the Boltzmann constant; and T is the absolute temperature. Impingement rates ($c[k_B T/2\pi m]^{1/2}$) of a liquid upon a solid surface are on the order of 10^{30} m^{-2} s^{-1} as compared to roughly 10^{19} surface atoms m^{-2}. That is, there are roughly 10^{11} collisions per second per surface atom. The sticking coefficients of fluoride and water on empty sites should both be close to unity. Hence, empty sites should fill rapidly at a surface and cannot have a coverage that exceeds the coverage of either F(a) or OH(a). These coverages must all be below a few percent of a monolayer in the pore formation regime since these species are not detected by FTIR either during anodic[119,120] or after stain etching.[103] During anodization in the electropolishing regime, oxide has been detected.[121,122]

From eqs 11 and 12, the ratio of the rate of H_2O adsorption to F^- adsorption is

$$R_{wF} = \frac{s_w c_w}{s_F c_F}\left[\frac{m_F}{m_w}\right]^{1/2} \theta^* \tag{13}$$

The hydroxide units formed by water dissociation can lead to the formation of an oxide layer. The rate of oxide formation will be less than the rate of water dissociation because OH(a) is subject to ligand exchange with F^-(aq). Oxide formation occurs through the condensation of neighboring adsorbed OH groups[123−128] into Si−O−Si bridge bonds according to a field-assisted growth mechanism.[129] This reaction is self-limiting; that is, the rate decreases as the oxide layer thickness increases because of increased difficulty of getting the reactive species to the advancing oxide/Si interface.

As stated above, the number of empty sites will be directly proportional to the rate of hole injection. Therefore, the number of empty (or excited) sites will be directly proportional to oxidant concentration in stain etching, to bias voltage in anodic etching and H_2O_2 concentration in metal-assisted etching with hydrogen peroxide. Figure 6 shows the results of a calculation of R_{wF} in which $s_w c_w/s_F c_F$ is arbitrarily set to 50 (consistent with water having a higher concentration in an aqueous solution). Under the conditions used by Koker and Kolasinski[92,107] for laser-assisted etching, a steady-state coverage of holes of $\sim 1 \times 10^{-7}$ ML was calculated. While we do not know this value under stain etching conditions, in the region where $\theta^* \ll 0.01$ the rate of F^- adsorption clearly exceeds the rate of water dissociation, and this will correspond to the por-Si formation regime. However, at some critical value of θ^*, R_w will exceed R_F; eventually oxide formation will proceed faster than etching according to the Gerischer mechanism; and electropolishing will occur. Similarly, one should expect that in solutions that are sufficiently dilute in fluoride at some point water dissociation will be faster, and there should be some detectable oxide as has been observed during anodic dissolution in dilute solutions.[130]

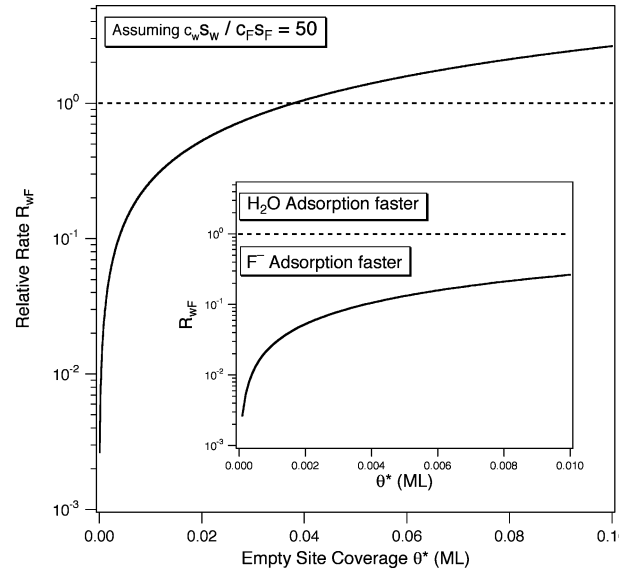

Figure 6. Rate of water adsorption relative to the rate of F^- adsorption. R_{wF} is plotted as a function of empty (or excited) site coverage θ^*. Since θ^* is directly proportional to the rate of hole injection, a transition from pore formation in the region of fast F^- adsorption (in which the curve lies below the dotted line) to electropolishing in the region of fast H_2O adsorption (above the dotted line) follows naturally from the described reaction dynamics.

The observed transition from por-Si formation to electropolishing can be explained within the dynamics described here. Furthermore, another requirement for a successful stain etchant can be stated as a sufficiently high ratio of the concentration of fluoride species relative to oxidant such that the hole injection rate is not so fast as to favor water adsorption over that of fluoride. This will ensure that oxide formation is slow or nonexistent.

From the above introduced arguments, there are several other requirements that we can develop for effective stain etching. The oxidant has to dissolve in the fluoride solution. It should not produce gas or an insoluble precipitate when it is reduced. For instance, MnO_4^- effectively injects holes and promotes por-Si formation,[60] but its counterion—particularly if it is K^+—can lead to precipitation of a hexafluorosilicate.[131] The charge transfer kinetics of the oxidant has to be suitable in terms of both rate and isotropy. It appears that neither perchlorate nor chromate produce por-Si or at least that they are very inefficient at doing so.[60,109] In the case of perchlorate, this may be because

of poor charge transfer kinetics. In the case of chromate, which is often used to expose defects on silicon surfaces, there may be some feature of the charge transfer reaction that favors anisotropic hole injection; i.e., it is better at injecting charge at defects and steps than terrace sites.

III. Conclusions

When silicon is exposed to an aqueous fluoride solution, a number of surface reactions can occur and the morphology of the etched surface depends sensitively on the balance of these reactions. Oxidation by water dissociation or step flow etching initiated by OH^- both favor the formation of uniform surfaces, whereas direct Si atom dissolution via the Gerischer mechanism favors porous silicon formation. Surface chemistry alone does not lead to porous silicon formation. It must be coupled to charge carrier dynamics to form a porous film. From a comprehensive analysis of the physical and chemical phenomena involved in the spontaneous etching of silicon in a fluoride + oxidant solution, seven requirements for the formulation of an effective stain etchant have been derived: (1) an acidic fluoride solution, (2) sufficiently high fluoride concentration compared to the oxidant concentration, (3) the oxidant must be able to inject holes into the Si valence band, thus its standard electrode potential should be more positive than approximately +0.7 V, (4) oxide formation needs to be slow or nonexistent, (5) the oxidant is soluble, and reduction of the oxidant leads to soluble products, (6) film homogeneity is enhanced if the oxidant's half-reaction does not evolve gas, and finally (7) the net etching reaction from hole injection to Si atom removal has to be sufficiently anisotropic (attacking all kinds of sites but only at the bottom of the pore) to support pore nucleation and propagation. On the basis of these requirements, stain etchants using Fe^{3+}, Ce^{4+}, and VO_2^+ have been formulated and shown to be highly effective at producing nanocrystalline porous silicon.

Acknowledgment. This work has been supported by West Chester University, the Center for Microanalysis and Imaging Research and Training (CMIRT), and the Pennsylvania State System of Higher Education (PASSHE).

References and Notes

(1) Kamat, P. V. *J. Phys. Chem. C* **2007**, *111*, 2834.
(2) Hochbaum, A. I.; Yang, P. D. *Chem. Rev.* **2010**, *110*, 527.
(3) Aricò, A. S.; Bruce, P.; Scrosati, B.; Tarascon, J. M.; Van Schalkwijk, W. *Nat. Mater.* **2005**, *4*, 366.
(4) Striemer, C. C.; Fauchet, P. M. *Phys. Status Solidi A* **2003**, *197*, 502.
(5) Aouida, S.; Saadoun, M.; Boujmil, M. F.; Ben Rabha, M.; Bessaïs, B. *Appl. Surf. Sci.* **2004**, *238*, 193.
(6) Peng, K.; Xu, Y.; Wu, Y.; Yan, Y.; Lee, S.-T.; Zhu, J. *Small* **2005**, *1*, 1062.
(7) Hassen, M.; Ben Jaballah, A.; Hajji, M.; Khedher, N.; Bessaïs, B.; Ezzaouia, H.; Rahmouni, H.; Ouaja, F. R.; Selmi, A. *Sol. Energy Mater.* **2005**, *87*, 493.
(8) Khedher, N.; Hajji, M.; Hassen, M.; Ben Jaballah, A.; Ouertani, B.; Ezzaouia, H.; Bessaïs, B.; Selmi, A.; Bennaceur, R. *Sol. Energy Mater.* **2005**, *87*, 605.
(9) Hajji, M.; Ben Jaballah, A.; Hassen, M.; Khedher, N.; Rahmouni, H.; Bessaïs, B.; Ezzaouia, H.; Selmi, A.; Bouchriha, H. *J. Mater. Sci.* **2005**, *40*, 1419.
(10) Khedher, N.; Ben Jaballah, A.; Hassen, M.; Hajji, M.; Ezzaouia, H.; Bessaïs, B.; Selmi, A.; Bennaceur, R. *Mater. Sci. Semicond. Process.* **2004**, *7*, 439.
(11) Yerokhov, V. Y.; Melnyk, I. I. *Renewable Sustainable Energy Rev.* **1999**, *3*, 291.
(12) Solanki, C. S.; Carnel, L.; Van Nieuwenhuysen, K.; Ulyashin, A.; Posthuma, N.; Beaucarne, G.; Poortmans, J. *Prog. Photovoltaics* **2005**, *13*, 201.
(13) Duerinckx, F.; Van Nieuwenhuysen, K.; Kim, H. J.; Kuzma-Filipek, I.; Beaucarne, G.; Poortmans, J. *Proc. 20th Eur. Photovoltaic Solar Energy Conf.* **2005**, 1190.
(14) Salonen, J.; Kaukonen, A. M.; Hirvonen, J.; Lehto, V. P. *J. Pharm. Sci.* **2008**, *97*, 632.
(15) Salonen, J.; Lehto, V. P. *Chem. Eng. J.* **2008**, *137*, 162.
(16) Ozdemir, S.; Gole, J. L. *Curr. Opin. Solid State Mater. Sci.* **2007**, *11*, 92.
(17) Tsubaki, K.; Yamanaka, H.; Kitada, K.; Komoda, T.; Koshida, N. *Jpn. J. Appl. Phys., Part 1* **2005**, *44*, 4436.
(18) Lillis, B.; Jungk, C.; Iacopino, D.; Whelton, A.; Hurley, E.; Sheehan, M. M.; Splinter, A.; Quinn, A.; Redmond, G.; Lane, W. A.; Mathewson, A.; Berney, H. *Biosens. Bioelectron.* **2005**, *21*, 282.
(19) Koshida, N.; Matsumoto, N. *Mater. Sci. Eng., R* **2003**, *40*, 169.
(20) Steiner, P.; Lang, W. *Thin Solid Films* **1995**, *255*, 52.
(21) Melnikov, V. A.; Astrova, E. V.; Perova, T. S.; Srigengan, V. *J. Micromech. Microeng.* **2008**, *18*, 025019.
(22) Yamamura, K.; Mitani, T. *Surf. Interface Anal.* **2008**, *40*, 1011.
(23) Teva, J.; Davis, Z. J.; Hansen, O. *J. Micromech. Microeng.* **2010**, *20*, 015034.
(24) Verplanck, N.; Coffinier, Y.; V., T.; Boukherroub, R. *Nanoscale Res. Lett.* **2007**, *2*, 577.
(25) Liu, Y. H.; Wang, X. K.; Luo, J. B.; Lu, X. C. *Appl. Surf. Sci.* **2009**, *255*, 9430.
(26) Cao, M. W.; Song, X. Y.; Zhai, J.; Wang, J. B.; Wang, Y. L. *J. Phys. Chem. B* **2006**, *110*, 13072.
(27) Kang, D. K.; Corno, J. A.; Gole, J. L.; Shin, H. C. *J. Electrochem. Soc.* **2008**, *155*, A276.
(28) Kim, H.; Han, B.; Choo, J.; Cho, J. *Angew. Chem., Int. Ed. Engl.* **2008**, *47*, 10151.
(29) Peng, K. Q.; Jie, J. S.; Zhang, W. J.; Lee, S. T. *Appl. Phys. Lett.* **2008**, *93*, 033105.
(30) Peng, K. Q.; Wang, X.; Lee, S. T. *Appl. Phys. Lett.* **2008**, *92*, 163103.
(31) Peng, K. Q.; Wang, X.; Wu, X. L.; Lee, S. T. *Nano Lett.* **2009**, *9*, 3704.
(32) Peng, K. Q.; Wang, X.; Lee, S. T. *Appl. Phys. Lett.* **2009**, *95*, 243112.
(33) Kolasinski, K. W. *Curr. Opin. Solid State Mater. Sci.* **2005**, *9*, 73.
(34) Dimova-Malinovska, D.; Sendova-Vassileva, M.; Tzenov, N.; Kamenova, M. *Thin Solid Films* **1997**, *297*, 9.
(35) Ashruf, C. M. A.; French, P. J.; Bressers, P. M. M. C.; Kelly, J. J. *Sens. Actuators, A* **1999**, *74*, 118.
(36) Xia, X. H.; Ashruf, C. M. A.; French, P. J.; Kelly, J. J. *Chem. Mater.* **2000**, *12*, 1671.
(37) Li, X.; Bohn, P. W. *Appl. Phys. Lett.* **2000**, *77*, 2572.
(38) Harada, Y.; Li, X.; Bohn, P. W.; Nuzzo, R. G. *J. Am. Chem. Soc.* **2001**, *123*, 8709.
(39) Chattopadhyay, S.; Li, X.; Bohn, P. W. *J. Appl. Phys.* **2002**, *91*, 6134.
(40) Chattopadhyay, S.; Bohn, P. W. *J. Appl. Phys.* **2004**, *96*, 6888.
(41) Splinter, A.; Stürmann, J.; Benecke, W. *Mater. Sci. Eng., C* **2001**, *15*, 109.
(42) Gorostiza, P.; Díaz, R.; Kulandainathan, M. A.; Sanz, F.; Morante, J. R. *J. Electroanal. Chem.* **1999**, *469*, 48.
(43) Gorostiza, P.; Anbu Kulandainathan, M.; Díaz, R.; Sanz, F.; Allongue, P.; Morante, J. R. *J. Electrochem. Soc.* **2000**, *147*, 1026.
(44) Gorostiza, P.; Allongue, P.; Díaz, R.; Morante, J. R.; Sanz, F. *J. Phys. Chem. B* **2003**, *107*, 6454.
(45) Chartier, C.; Bastide, S.; Levy-Clement, C. *Electrochim. Acta* **2008**, *53*, 5509.
(46) Peng, K.-Q.; Yan, Y.-J.; Gao, S.-p.; Zhu, J. *Adv. Mater.* **2002**, *14*, 1164.
(47) Peng, K.; Yan, Y.; Gao, S.; Zhu, J. *Adv. Funct. Mater.* **2003**, *13*, 127.
(48) Peng, K. Q.; Huang, Z. P.; Zhu, J. *Adv. Mater.* **2004**, *16*, 73.
(49) Peng, K. Q.; Wu, Y.; Fang, H.; Zhong, X. Y.; Xu, Y.; Zhu, J. *Angew. Chem., Int. Ed. Engl.* **2005**, *44*, 2737.
(50) Peng, K. Q.; Hu, J. J.; Yan, Y. J.; Wu, Y.; Fang, H.; Xu, Y.; Lee, S. T.; Zhu, J. *Adv. Funct. Mater.* **2006**, *16*, 387.
(51) Peng, K. Q.; Zhang, M. L.; Lu, A. J.; Wong, N. B.; Zhang, R. Q.; Lee, S. T. *Appl. Phys. Lett.* **2007**, *90*, 163123.
(52) Chan, C. K.; Peng, H. L.; Liu, G.; McIlwrath, K.; Zhang, X. F.; Huggins, R. A.; Cui, Y. *Nature Nanotechnol.* **2008**, *3*, 31.
(53) Zhang, M.-L.; Peng, K.-Q.; Fan, X.; Jie, J.-S.; Zhang, R.-Q.; Lee, S.-T.; Wong, N.-B. *J. Phys. Chem. C* **2008**, *112*, 4444.
(54) Peng, K. Q.; Lu, A. J.; Zhang, R. Q.; Lee, S. T. *Adv. Func. Mater.* **2008**, *18*, 3026.
(55) Peng, K. Q.; Wang, X.; Wu, X. L.; Lee, S. T. *Appl. Phys. Lett.* **2009**, *95*, 143119.
(56) Robbins, H.; Schwartz, B. *J. Electrochem. Soc.* **1959**, *106*, 505.
(57) Robbins, H.; Schwartz, B. *J. Electrochem. Soc.* **1960**, *107*, 108.

(58) Robbins, H.; Schwartz, B. *J. Electrochem. Soc.* **1961**, *108*, 365.
(59) Turner, D. R. *J. Electrochem. Soc.* **1960**, *107*, 810.
(60) Nahidi, M.; Kolasinski, K. W. *J. Electrochem. Soc.* **2006**, *153*, C19.
(61) Peng, K. Q.; Zhu, J. *Electrochim. Acta* **2004**, *49*, 2563.
(62) Peng, K. Q.; Fang, H.; Hu, J. J.; Wu, Y.; Zhu, J.; Yan, Y. J.; Lee, S. *Chem.—Eur. J.* **2006**, *12*, 7942.
(63) Tsujino, K.; Matsumura, M. *Electrochem. Solid State Lett.* **2005**, *8*, C193.
(64) Tsujino, K.; Matsumura, M. *Adv. Mater.* **2005**, *17*, 1045.
(65) Lehmann, V. *Electrochemistry of Silicon: Instrumentation, Science, Materials and Applications*; Wiley-VCH: Weinheim, 2002.
(66) Carstensen, J.; Christophersen, M.; Föll, H. *Mater. Sci. Eng., B* **2000**, *69−70*, 23.
(67) Föll, H.; Christophersen, M.; Carstensen, J.; Hasse, G. *Mater. Sci. Eng., R* **2002**, *39*, 93.
(68) Smith, R. L.; Collins, S. D. *J. Appl. Phys.* **1992**, *71*, R1.
(69) Langa, S.; Carstensen, J.; Christophersen, M.; Steen, K.; Frey, S.; Tiginyanu, I. M.; Föll, H. *J. Electrochem. Soc.* **2005**, *152*, C525.
(70) Macak, J. M.; Tsuchiya, H.; Ghicov, A.; Yasuda, K.; Hahn, R.; Bauer, S.; Schmuki, P. *Curr. Opin. Solid State Mater. Sci.* **2007**, *11*, 3.
(71) Chik, H.; Xu, J. M. *Mater. Sci. Eng., R* **2004**, *43*, 103.
(72) Lehmann, V.; Gösele, U. *Appl. Phys. Lett.* **1991**, *58*, 856.
(73) Gerischer, H. Principles of Electrochemistry. In *The CRC Handbook of Solid State Electrochemistry*; Gellings, P., Bouwmeester, H., Eds.; CRC Press: Boca Raton, 1997; p 9.
(74) van Buuren, T.; Dinh, L. N.; Chase, L. L.; Siekhaus, W. J.; Terminello, L. J. *Phys. Rev. Lett.* **1998**, *80*, 3803.
(75) Cullis, A. G.; Canham, L. T.; Calcott, P. D. J. *J. Appl. Phys.* **1997**, *82*, 909.
(76) Morrison, S. R. *Electrochemistry at Semiconductor and Oxidized Metal Electrodes*; Plenum: New York, 1980.
(77) Lundqvist, B. I.; Hellman, A.; Zorić, I. Electron Transfer and Nonadiabaticity. In *Handbook of Surface Science: Dynamics*; Hasselbrink, E., Lundqvist, I., Eds.; Elsevier: Amsterdam, 2008; Vol. 3; p 429.
(78) *CRC Handbook of Chemistry and Physics*; 91st ed.; Haynes, W. M., Ed.; CRC Press: Boca Raton, FL, 2010; Vol. 91.
(79) Good, W. D.; Lacina, J. L.; DePrater, B. L.; McCullough, J. P. *J. Phys. Chem.* **1964**, *68*, 579.
(80) Judge, J. S. *J. Electrochem. Soc.* **1971**, *118*, 1772.
(81) Zhang, R. Q.; Zhao, Y. L.; Teo, B. K. *Phys. Rev. B* **2004**, *69*, 125319.
(82) Halimaoui, A. *Surf. Sci.* **1994**, *306*, L550.
(83) Hu, S. M.; Kerr, D. R. *J. Electrochem. Soc.* **1967**, *114*, 414.
(84) Proksche, H.; Nagorsen, G.; Ross, D. *J. Electrochem. Soc.* **1992**, *139*, 521.
(85) Ubara, H.; Imura, T.; Hiraki, A. *Solid State Commun.* **1984**, *50*, 673.
(86) Burrows, V. A.; Chabal, Y. J.; Higashi, G. S.; Raghavachari, K.; Christman, S. B. *Appl. Phys. Lett.* **1988**, *53*, 998.
(87) Baum, T.; Schiffrin, D. J. *J. Chem. Soc., Faraday Trans.* **1998**, *94*, 691.
(88) Allongue, P.; Costa-Kieling, V.; Gerischer, H. *J. Electrochem. Soc.* **1993**, *140*, 1009.
(89) Allongue, P.; Costa-Kieling, V.; Gerischer, H. *J. Electrochem. Soc.* **1993**, *140*, 1018.
(90) Faggin, M. F.; Green, S. K.; Clark, I. T.; Queeney, K. T.; Hines, M. A. *J. Am. Chem. Soc.* **2006**, *128*, 11455.
(91) Hines, M. A. *Annu. Rev. Phys. Chem.* **2003**, *54*, 29.
(92) Kolasinski, K. W. *Phys. Chem. Chem. Phys.* **2003**, *5*, 1270.
(93) Jakob, P.; Chabal, Y. J.; Raghavachari, K.; Becker, R. S.; Becker, A. J. *Surf. Sci.* **1992**, *275*, 407.
(94) Allongue, P.; Kieling, V.; Gerischer, H. *Electrochim. Acta* **1995**, *40*, 1353.
(95) Allongue, P.; Henry de Villeneuve, C.; Morin, S.; Boukherroub, R.; Wayner, D. D. M. *Electrochim. Acta* **2000**, *45*, 4591.
(96) Munford, M. L.; Cortes, R.; Allongue, P. *Sens. Mater.* **2001**, *13*, 259.
(97) Zanoni, R.; Righini, G.; Mattogno, G.; Schirone, L.; Sotgiu, G.; Rallo, F. *J. Lumin.* **1998**, *80*, 159.
(98) Steinert, M.; Acker, J.; Henssge, A.; Wetzig, K. *J. Electrochem. Soc.* **2005**, *152*, C843.
(99) Steinert, M.; Acker, J.; Krause, M.; Oswald, S.; Wetzig, K. *J. Phys. Chem. B* **2006**, *110*, 11377.
(100) Steinert, M.; Acker, J.; Oswald, S.; Wetzig, K. *J. Phys. Chem. C* **2007**, *111*, 2133.
(101) Steinert, M.; Acker, J.; Wetzig, K. *J. Phys. Chem. C* **2008**, *112*, 14139.
(102) Lewerenz, H. J.; Aggour, M.; Murrell, C.; Kanis, M.; Jungblut, H.; Jakubowicz, J.; Cox, P. A.; Campbell, S. A.; Hoffmann, P.; Schmeisser, D. *J. Electrochem. Soc.* **2003**, *150*, E185.
(103) Kolasinski, K. W.; Hartline, J. D.; Kelly, B. T.; Yadlovskiy, J. *Mol. Phys.* **2010**, *108*, 1033.
(104) Kolasinski, K. W. *Surf. Sci.* **2009**, *603*, 1904.
(105) Kolasinski, K. W. Growth and Etching of Semiconductors. In *Handbook of Surface Science: Dynamics*; Hasselbrink, E., Lundqvist, I., Eds.; Elsevier: Amsterdam, 2008; Vol. 3; p 787.
(106) Kooij, E. S.; Butter, K.; Kelly, J. J. *Electrochem. Solid State Lett.* **1999**, *2*, 178.
(107) Koker, L.; Kolasinski, K. W. *J. Phys. Chem. B* **2001**, *105*, 3864.
(108) Dudley, M. E.; Kolasinski, K. W. *Phys. Status Solidi A* **2009**, *206*, 1240.
(109) Dudley, M. E.; Kolasinski, K. W. *Electrochem. Solid State Lett.* **2009**, *12*, D22.
(110) Lee, C.; Koker, L.; Kolasinski, K. W. *Appl. Phys. A: Mater. Sci. Process.* **2000**, *71*, 77.
(111) Kolasinski, K. W.; Aindow, M.; Barnard, J. C.; Ganguly, S.; Koker, L.; Wellner, A.; Palmer, R. E.; Field, C.; Hamley, P.; Poliakoff, M. *J. Appl. Phys.* **2000**, *88*, 2472.
(112) Hamilton, B.; Jacobs, J.; Hill, D. A.; Pettifer, R. F.; Teehan, D.; Canham, L. T. *Nature (London)* **1998**, *393*, 443.
(113) Zhang, X. G.; Collins, S. D.; Smith, R. L. *J. Electrochem. Soc.* **1989**, *136*, 1561.
(114) Chazalviel, J. N.; Ozanam, F. *J. Electrochem. Soc.* **1992**, *139*, 2501.
(115) Ozanam, F.; Blanchard, N.; Chazalviel, J. N. *Electrochim. Acta* **1993**, *38*, 1627.
(116) Lewerenz, H. J. *J. Phys. Chem. B* **1997**, *101*, 2421.
(117) Grzanna, J.; Notz, T.; Lewerenz, H. J. *Phys. Status Solidi C* **2009**, *6*, 1639.
(118) Grzanna, J.; Notz, T.; Lewerenz, H. J. *ECS Trans.* **2008**, *16*, 173.
(119) Rao, A. V.; Ozanam, F.; Chazalviel, J.-N. *J. Electrochem. Soc.* **1991**, *138*, 153.
(120) Chazalviel, J.-N.; Ozanam, F. *J. Appl. Phys.* **1997**, *81*, 7684.
(121) da Fonseca, C.; Ozanam, F.; Chazalviel, J.-N. *Surf. Sci.* **1996**, *365*, 1.
(122) Safi, M.; Chazalviel, J.-N.; Cherkaoui, M.; Belaïdi, A.; Gorochov, O. *Electrochim. Acta* **2002**, *47*, 2573.
(123) Bressers, P. M. M. C.; Pagano, S. A. S. P.; Kelly, J. J. *J. Electroanal. Chem.* **1995**, *391*, 159.
(124) Bressers, P. M. M. C.; Kelly, J. J.; Gardeniers, J. G. E.; Elwenspoek, M. *J. Electrochem. Soc.* **1996**, *143*, 1744.
(125) Gräf, D.; Grundner, M.; Schulz, R. *J. Vac. Sci. Technol., A* **1989**, *7*, 808.
(126) Ogata, Y. H.; Kato, F.; Tsuboi, T.; Sakka, T. *J. Electrochem. Soc.* **1998**, *145*, 2439.
(127) Ogata, Y.; Niki, H.; Sakka, T.; Iwasaki, M. *J. Electrochem. Soc.* **1995**, *142*, 1595.
(128) Gupta, P.; Dillon, A. C.; Bracker, A. S.; George, S. M. *Surf. Sci.* **1991**, *245*, 360.
(129) Neuwald, U.; Feltz, A.; Memmert, U.; Behm, R. J. *J. Appl. Phys.* **1995**, *78*, 4131.
(130) Belaïdi, A.; Safi, M.; Ozanam, F.; Chazalviel, J.-N.; Gorochov, O. *J. Electrochem. Soc.* **1999**, *146*, 2659.
(131) Koker, L.; Wellner, A.; Sherratt, P. A. J.; Neuendorf, R.; Kolasinski, K. W. *J. Phys. Chem. B* **2002**, *106*, 4424.